Journal of The Electrochemical Society, **157** (9) D496-D499 (2010)
0013-4651/2010/157(9)/D496/4/$28.00 © The Electrochemical Society

Fabrication of Deep Si Trenches by Self-Assembled Wet Chemical Etching Process

S. C. Hung,[a] S. C. Shiu,[a] J. J. Chao,[a] and C. F. Lin[a,b,z]

[a]*Graduate Institute of Photonics and Optoelectronics and* [b]*Graduate Institute of Electronics Engineering and Department of Electrical Engineering, National Taiwan University, Taipei 10617, Taiwan*

This paper describes a method for fabricating deep Si trenches with only a wet chemical etching process. A typical photolithography process was used to define the etching area. Aqueous $HF/AgNO_3$ and HF/H_2O_2 solutions were applied to etch silicon nanowire (SiNW) structures in the selected domains. In the former case, a high selectivity between the bare Si surface and photoresist-covered Si surface can be achieved. The SiNWs with a monolithic ⟨100⟩ direction can be etched in the selected domain. However, additional ⟨010⟩- and ⟨001⟩-oriented etchings were observed on the trench sidewall and wafer surface in the latter case. In addition, deep and highly anisotropic trenches were achieved by removing the SiNWs. The Si wafer was immersed in a concentrated aqueous HF/H_2O_2 solution. A porous structure was formed in the vicinity of Ag nanoparticles, suggesting that one should remove SiNWs completely to achieve deep anisotropic trenches. This method exhibits high anisotropy and is capable of etching deep Si trenches with depths of about 50 μm without an additional etching mask. It effectively minimizes instrument costs and reveals the potential of large-area fabrication.
 [DOI: 10.1149/1.3462976]

Manuscript received April 14, 2010. Published July 16, 2010.

High anisotropy in Si etching is required in various applications. For example, semiconductor devices, including optical biosensors,[1] optical switches,[2] and metal-oxide-semiconductor field effect transistor devices,[3] require the formation of silicon trenches at some point in their fabrication. These trench dimensions typically range from 1 to 4 μm in width and 0.5–5 μm in depth. However, during the fabrication of microelectromechanical systems,[4] the patterning of silicon is an essential step. Deep Si trenches with depths between 10 and 100 μm are demanded. Furthermore, recently ultrathin Si solar microcells[5] have received increasing attention due to the reduction of material consumption. Pre-etching with depths of around 10 μm in the vertical direction is required for wafer slicing.

Numerous methods were studied in fabricating Si trenches, including reactive ion etching (RIE), KOH wet chemical etching, and laser-assisted direct imprint (LADI).[6] However, these methods have several drawbacks. RIE is a typical method for creating highly anisotropic structures in conventional semiconductor fabrication, but it exploits expensive instruments and is rarely performed on an ultralarge scale. Moreover, an additional hard etching mask is needed for deep RIE. KOH wet chemical etching is a low cost and large-area fabrication method, but the etching direction is restricted by the crystal orientation. LADI is a rapid technique for patterning nanostructures in silicon that does not require etching. However, the fabrication linewidths and depths by LADI are limited to submicrometers. As a result, a low cost and large-area method for fabricating highly anisotropic Si trenches with dimensions from nanometers to micrometers should be developed.

Here, we present an alternative method for fabricating Si trenches using only wet chemical etching processes. A typical photolithography process was used to define the etching domain. Silicon nanowires (SiNWs) were etched in the selected area and removed by a chemical solution containing H_2O_2. In this paper, aqueous $HF/AgNO_3$ and HF/H_2O_2 solutions were applied to etch SiNW structures in the desired domains. Ag serving as reaction catalysts was prepared by electroless metal deposition (EMD) and thermal evaporation. In addition, the impact of etching widths and periods was investigated. Finally, a concentrated aqueous HF/H_2O_2 solution was used to remove SiNW structures. Through this method, deep and anisotropic Si trenches can be created.

Method

Figure 1 shows the diagram of this method. A p-type Si(100) wafer with a resistance of 1–10 Ω cm was used. The Si wafer was first spin coated with the photoresist and patterned using a typical photolithography process. The Ag catalysts were subsequently deposited through EMD or thermal evaporation. The Si wafer was then immersed in the etching solution. Aqueous $HF/AgNO_3$ [0.02 mol/L $AgNO_3$ and 10% HF in deionized (DI) water] and HF/H_2O_2 (0.6% H_2O_2 and 10% HF in DI water) solutions were applied to etch nanowire structures in the desired domains. In addition, to remove the nanowire structure, the wafer was immersed in a concentrated aqueous HF/H_2O_2 solution (2.4% H_2O_2 and 6.6% HF in DI water). Porous structures were formed in the vicinity of Ag nanoparticles, suggesting that one should remove SiNWs completely to achieve deep anisotropic trenches.

In this work, wet chemical etching was preferred on the (100) substrate. For the fabrication on the (110) and (111) substrates, the crystallographically preferred etching was along the ⟨100⟩ direction in Ref. 7-14. However, vertically aligned ⟨110⟩ and ⟨111⟩ SiNWs were also found on the (110) and (111) substrates, respectively, in Ref. 12 and 13. Furthermore, well-aligned ⟨110⟩ SiNWs were controlled by suppressing the crystallographically preferred ⟨100⟩ direction in Ref. 14. These works show the possibilities for etching vertical Si trenches on variously oriented wafers.

Self-Assembled Etching in Selected Area

Wet chemical etching using aqueous HF/AgNO$_3$ and HF/H$_2$O$_2$ solutions.— The etching selectivity between the bare Si surface and photoresist-covered Si surface highly depends on the chemical solutions used. To observe the selectivity in different chemical solutions, aqueous $HF/AgNO_3$ and HF/H_2O_2 solutions were applied. In the case using an aqueous $HF/AgNO_3$ solution, the lithography-defined samples were immersed in an aqueous $HF/AgNO_3$ solution (0.02 mol/L $AgNO_3$ and 10% HF in DI water) for 30 min. Figure 2a and b shows the scanning electron microscopy (SEM) images created using an aqueous $HF/AgNO_3$ solution. The domain-selective SiNWs present superior selectivity between the etching and nonetching domains. However, in the case using an aqueous HF/H_2O_2 solution, the samples were first immersed in the aqueous $HF/AgNO_3$ (0.02 mol/L $AgNO_3$ and 10% HF in DI water) solution for 20 s to deposit Ag nanoparticles and subsequently immersed in an aqueous HF/H_2O_2 solution (0.6% H_2O_2 and 10% HF in DI water) for 30 min. Figure 2c and d shows the SEM images created using an aqueous HF/H_2O_2 solution. The case using an aqueous HF/H_2O_2 solution exhibits significant surface damage in the nonetching domain. The etching directions of SiNWs are not only the ⟨100⟩ direction but also the ⟨010⟩ and ⟨001⟩ directions.

The reason for the difference in the above two cases is as fol-

[z] E-mail: cflin@cc.ee.ntu.edu.tw

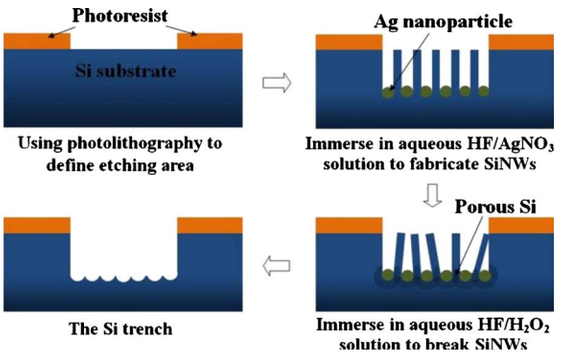

Figure 1. (Color online) The fabrication method of an anisotropic Si trench.

lows. Using the aqueous $HF/AgNO_3$ solution, the Ag ions in the solution deposit on the bare Si surface and dendritic structures of Ag nanoparticles are formed. Subsequently, the rest of the Ag ions in the solution prefer to accumulate on the dendritic structures to create a redox reaction. The Ag ions do not enter the trenches, accumulating to cause Si oxidization. This mode of etching is suitable for deep anisotropic trenches. However, using the aqueous HF/H_2O_2 solution, the sample is immersed in the aqueous HF/H_2O_2 solution after the initial Ag deposition. At this point, H_2O_2 in the solution causes two redox reactions. Except for the oxidization of Si via Ag catalysts, it leads to the deposited Ag nanoparticles becoming Ag ions. The resolved Ag ions are likely to deposit on the trench sidewalls and the wafer surface. This results in the ⟨010⟩- and ⟨001⟩-oriented etching of SiNWs.

Ag catalysts prepared by thermal evaporation.— In this section, Ag catalysts were prepared through thermal evaporation for comparison. First, a continuous strip-shaped Ag film was deposited by a lithography system and an E-beam evaporator. Subsequently, the samples were immersed in the aqueous HF/H_2O_2 solution (0.6% H_2O_2 and 10% HF in DI water) for 30 min to etch Si trenches. A similar method has been reported.[9,10] Here, Si trenches using this method with different widths are investigated. Figure 3a and b shows cross sections of the samples with widths of 500 nm and 5 μm, respectively. In Fig. 3a, the Si trench could be etched vertically, but the etching rate is extremely slow (about 1 μm/h). However, Fig. 3b shows a cross section of the samples with widths of 5 μm. The etching direction was greatly bended.

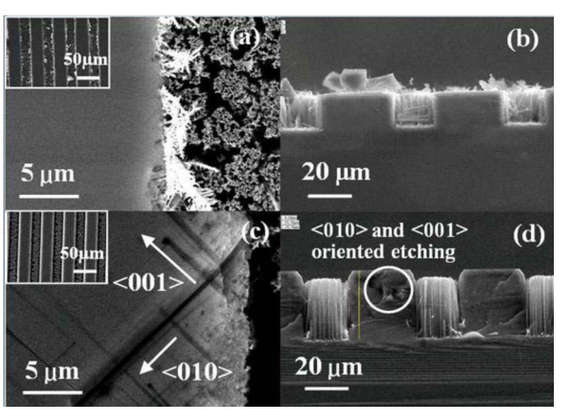

Figure 2. (Color online) The SEM images of the SiNWs in the selected area by using aqueous (a) $HF/AgNO_3$ and (c) HF/H_2O_2 solutions. Inserts in (a) and (c) are the images in large area. (b) and (d) are the corresponding cross sections in (a) and (c), respectively.

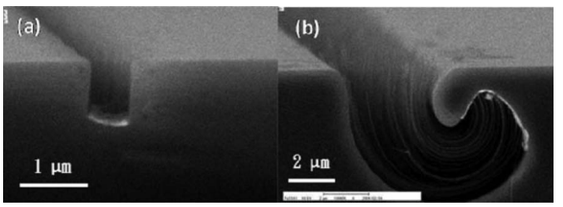

Figure 3. The SEM images of the samples with thermal evaporated Ag layers as the catalysts. The cross sections of the samples with etching widths of (a) 500 nm and (b) 5 μm.

The morphology in the two kinds of Ag catalysts leads to the different etching conditions. Using silver nanoparticles, the morphology of the particles with a diameter of about 30 nm allows HF to easily etch the SiO_2 layer. In this way, SiNWs are formed in the trenches. However, the morphology of stripes with linewidths above several hundreds of nanometers obstructs the HF solution from entering the area underneath the Ag layer. As a result, the etching rate is extremely slow. For a larger linewidth (above several micrometers), etching is only achieved when the Ag film has apertures. The random apertures in different areas result in different etching rates. The different etching rates and the interconnection of the Ag film create a greatly bended etching.

Influences of the etching widths and periods.— Material economization is the main issue in ultrathin crystalline Si solar cells.[5] A smaller Kerf loss indicates lower material consumption. The minimum etching width was investigated here. Figure 4a-e shows the results after 30 min of etching the samples with linewidths of 10 μm, 5 μm, 3 μm, 1 μm, and 500 nm, respectively. The inserts show the corresponding cross-sectional images. For 3 μm and above 3 μm, well-aligned SiNWs perpendicular to the substrate surface (100) were formed in the selected domain. Moreover, the etching depths were the same. However, for 1 μm and below 1 μm, irregular shapes were etched in the selected domain. The

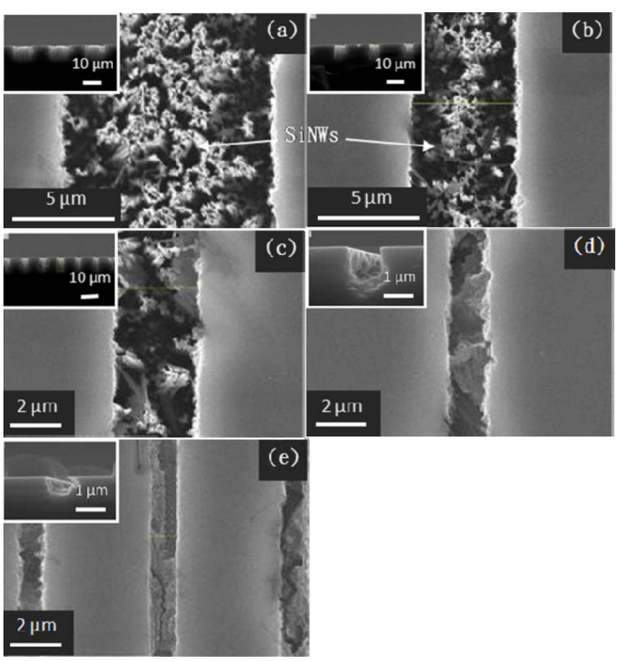

Figure 4. (Color online) The SEM images of the results for 30 min etching of the samples with linewidths of (a) 10 μm, (b) 5 μm, (c) 3 μm, (d) 1 μm, and (e) 500 nm, respectively. The inserts show the corresponding images of cross section.

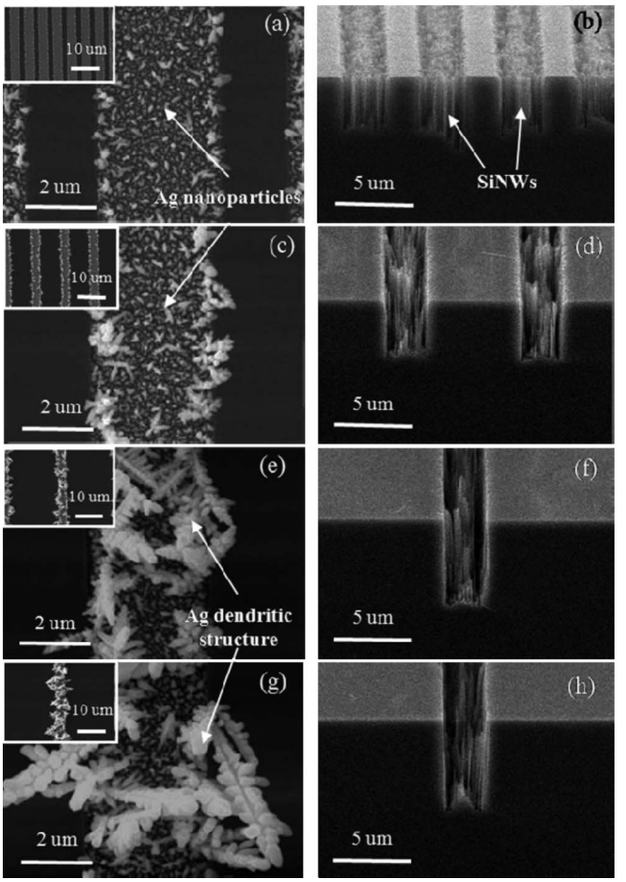

Figure 5. The SEM images of Ag deposition for 20 s with different periods. The etching linewidth for all samples is 3 μm and the periods of etching strip are (a) 5, (c) 10, (e) 20, and (g) 40 μm, respectively. The insert in each figure shows corresponding images in the large area. (b), (d), (f), and (h) are the corresponding SEM images of SiNWs etching in (a), (c), (e), and (g), respectively.

etching depths were much shallower than that with SiNWs. Additionally, the etching depth for 0.5 μm was even shallower than that for 1 μm width. The etching mechanism for SiNWs can be explained simply by two chemical reactions. One is a redox reaction (reduction: $Ag^+ + e^- \Rightarrow Ag$; oxidation: $Si + 2H_2O \Rightarrow SiO_2 + 2H^+ + 2e^-$) with Ag nanoparticles as the catalysts. The other is the etching of silicon oxide by the HF solution ($SiO_2 + 6HF \Rightarrow H_2SiF_6 + 2H_2O$). In the small-width cases, HF slowly permeates into the trenches to etch SiO_2. The SiO_2 around the Ag nanoparticles becomes an electron blocking layer. Consequently, the Ag ions are prohibited from continuing to accumulate on the SiO_2-clad Ag nanoparticles. This causes the regular SiNW etching to stop and Plank's motion[8] or a certain mechanism to dominate, resulting in an irregular shape.

For the etching solution with stationary concentration, the local size in the selected area affects the Ag deposition rate. In this experiment, the etching rate varied with the trenches' periods. The period here is defined as the summation of the trench width and the spacing between two trenches. The samples with a 3 μm etching domain were immersed in the aqueous $HF/AgNO_3$ solution for 20 s. Figure 5a, c, e, and g shows the samples with periods of 5, 10, 20, and 40 μm, respectively. Figure 5b, d, f, and h shows the corresponding SEM images of SiNW etching for 10 min. The depths of the Si trenches were estimated to be 2.8, 3.7, 5.4, and 5.6 μm for periods of 5, 10, 20, and 40 μm, respectively. Deeper Si trenches were found with increased periods. In addition, SiNWs' forming in the cases with larger periods was rarer. This indicates that the Ag nanoparticles were denser on the selected Si surface.

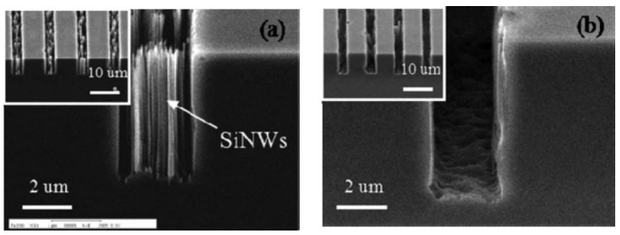

Figure 6. The SEM images of deep Si trenches by (a) using aqueous $HF/AgNO_3$ solution to selectively etch SiNWs and (b) subsequently using aqueous HF/H_2O_2 solution to remove SiNWs. The insert in each figure shows corresponding images in large area.

Si Trenches

Figure 6 shows SEM images of the fabrication of Si trenches. Figure 6a and b shows images of the samples before and after removing SiNWs, respectively. The SiNW structure was formed in the specific area. Deep and highly anisotropic trenches were achieved due to the self-assembled etching. However, the SiNWs were efficiently removed by the aqueous HF/H_2O_2 solution. The depth of the Si trenches was slightly larger after removing the SiNWs. The sidewall and the bottom of the trenches present roughness of about several tens of nanometers. This is due to the irregular morphology of Ag deposition. After removing the SiNWs, the roughness can be reduced. Various methods, including dry oxidation,[15] wet chemical oxidation,[16] hydrogen annealing,[17] and excimer laser reformation,[18] have been demonstrated to effectively reduce roughness.

Fast etching rate is one of the advantages of using wet chemical etching. The etching rate in this method depends on the process of SiNW etching, while the process of forming porous Si takes only tens of seconds. Figure 7 shows a diagram of etching depths vs etching time for the SiNW trenches of 20 μm in width and 50 μm in trench period. Inserts (a), (b), and (c) are the SEM images of SiNWs etching for 15, 45, and 75 min, respectively. The etching rate was about 30 μm/h.

Conclusion

The fabrication of deep Si trenches using a self-assembled wet chemical etching process is presented. Aqueous $HF/AgNO_3$ and HF/H_2O_2 solutions were applied to etch SiNW structures in the desired domains. When using an aqueous HF/H_2O_2 solution, ⟨010⟩- and ⟨001⟩-oriented etching was observed on the trench sidewall and

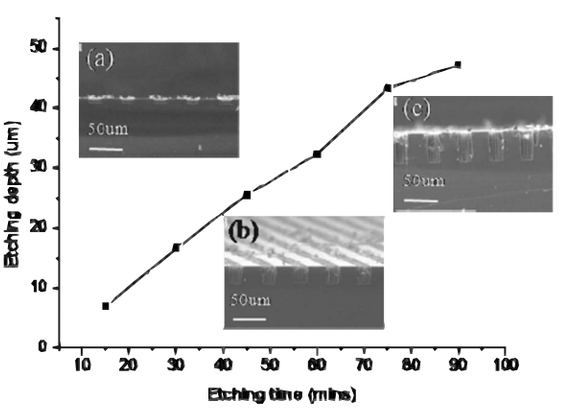

Figure 7. The etching rate: The figure shows the etching depth (μm) vs the etching time (min). (a), (b), and (c) are the images of cross section after etching for 15, 45, and 75 min, respectively.

wafer surface. This leads to undesired damage on the nonetching domain. However, high selectivity between the bare Si surface and photoresist-covered Si surface can be achieved using the aqueous $HF/AgNO_3$ solution. The Ag ions in this etching solution prefer to accumulate on self-assembled dendritic structures. This causes the SiNWs with a monolithic $\langle 100 \rangle$ direction to be etched in the selected domain. In addition, Ag catalysts were prepared by thermal evaporation for comparison. A continuous stripe-shaped Ag film was deposited through a lithography system and an E-beam evaporator. It exhibited an extremely slow etching rate. The morphology of the micrometer/submicrometer-width silver strips retarded the etching process. Finally, deep and highly anisotropic trenches were achieved by removing the SiNWs. The wafer was immersed in a concentrated aqueous HF/H_2O_2 solution. Porous structures were formed in the vicinity of Ag nanoparticles, suggesting that one should remove the SiNW completely to achieve deep anisotropic trenches. This method exhibits high anisotropy and is capable of etching deep Si trenches with depths of about 50 μm without an additional etching mask. It effectively minimized instrument costs and facilitated large-area fabrications.

Acknowledgments

This work was supported by the National Science Council, Taiwan with grant no. NSC96-2221-E-002-277-MY3, no. NSC97-2218-E-002-013, and no. NSC97-2221-E-002-039-MY3.

National Taiwan University assisted in meeting the publication costs of this article.

References

1. F. Prieto, B. Sepúlveda, A. Calle, A. Llobera, C. Domínguez, A. Abad, A. Montoya, and L. M. Lechuga, *Nanotechnology*, **14**, 907 (2003).
2. V. R. Almeida and M. Lipson, *Opt. Lett.*, **29**, 2387 (2004).
3. D. J. Frank, R. H. Dennard, E. Nowak, P. M. Solomon, Y. Taur, and H.-S. P. Wong, *Proc. IEEE*, **89**, 259 (2001).
4. K. Kuhl, S. Vogel, U. Schaber, R. Schafflik, and B. Hillrich, in *SPIE Conference on Micromachining and Microfabrication Process Technology*, pp. 97–105 (1998).
5. J. Yoon, A. J. Baca, S.-I. Park, P. Elvikis, J. B. Geddes, III, L. Li, R. Hwan Kim, J. Xiao, S. Wang, T.-H. Kim, et al., *Nature Mater.*, **7**, 907 (2008).
6. S. Y. Chou, C. Keimel, and J. Gu, *Nature*, **417**, 835 (2002).
7. K.-Q. Peng, Y.-J. Yan, S.-P. Gao, and J. Zhu, *Adv. Mater.*, **14**, 1164 (2002).
8. K. Q. Peng, Z. P. Huang, and J. Zhu, *Adv. Mater.*, **16**, 73 (2004).
9. K.-Q. Peng, Y. Xu, Y. Wu, Y. Yan, S.-T. Lee, and J. Zhu, *Small*, **1**, 1062 (2005).
10. K. Q. Peng, J. J. Hu, Y. J. Yan, Y. Wu, H. Fang, Y. Xu, S. T. Lee, and J. Zhu, *Adv. Funct. Mater.*, **16**, 387 (2006).
11. K.-Q. Peng, X. Wang, and S.-T. Lee, *Appl. Phys. Lett.*, **92**, 163103 (2008).
12. K.-Q. Peng, A. Lu, R. Zhang, and S.-T. Lee, *Adv. Funct. Mater.*, **18**, 3026 (2008).
13. C.-Y. Chen, C.-S. Wu, C.-J. Chou, and T.-J. Yen, *Adv. Mater.*, **20**, 3811 (2008).
14. Z.-P. Huang, T. Shimizu, S. Senz, Z. Zhang, X. Zhang, W. Lee, N. Geyer, and U. Gosele, *Nano Lett.*, **9**, 2519 (2009).
15. J. Takahashi, T. Tsuchizawa, T. Watanabe, and S. Itabashi, *J. Vac. Sci. Technol. B*, **22**, 2522 (2004).
16. D. K. Sparacin, S. J. Spector, and L. C. Kimerling, *J. Lightwave Technol.*, **23**, 2455 (2005).
17. H. Kuribayashi, R. Hiruta, R. Shimizu, K. Sudoh, and H. Iwasaki, *J. Vac. Sci. Technol. A*, **21**, 1279 (2003).
18. S.-H. Hung, E.-Z. Liang, and C.-F. Lin, *J. Lightwave Technol.*, **27**, 887 (2009).